

A DYNAMIC FRICTION MODEL FOR REACTION WHEELS

Valdemir Carrara^{*}, Adolfo Graciano da Silva[†] and Hélio Koiti Kuga[‡]

This paper addresses the problem of the bearing friction in a reaction wheel and applies a dynamic friction model in the current control loop. The dynamic friction model assumes that there are elastic bristles in the contact surfaces that bends when slipping forces are applied. The bristle behavior mimics the Stribeck effect without discontinuities. Some experiments were carried out in order to collect the necessary data to estimate the model parameters, using different control profiles in both current and velocity so as to emphasize a particular parameter. Least squares curve fitting was firstly employed to obtain viscous and Coulomb friction coefficients, while a Kalman filter estimated the break-away torque for a Stribeck friction model as well as viscous and Coulomb. Finally an Extended Kalman Filter (EKF) was used to obtain some parameters of a LuGre dynamic friction model. Results of the filtering process are presented, thus asserting that dynamic friction models can be estimated with EKF provided the necessary conditions for sensor accuracy are met.

INTRODUCTION

Reaction wheels (RW) are largely employed for satellite attitude control, from small micro-satellites to large ones. Its ability to deliver a broad range of torques, to operate in continuous increment of angular velocities and to be powered by a non-consumable energy source, besides high reliability, makes them suitable for attitude stabilization and control. Even considering that attitude control with reaction wheels demands an external torque generator (magnetic torque coils or thrusters, to say the most common), they are the best choice when 3-axis stabilization and fine attitude pointing are required. Reaction wheels are complex devices and they usually hide inside a huge amount of technology and design effort necessary to produce them. A reaction wheel comprises a flywheel of large inertia and low mass in small volume (which are, of course, incompatible requirements), a brushless DC motor, a sealed housing, the shaft and bearings, a tachometer or a angular measurement system like an optical encoder, for instance, and, not less important, the electronics and communication hardware. The electronics provide motor drive and commutation, tacho readouts, speed and temperature monitoring (sometimes also the internal pressure), command decoding, telemetry packing and delivering, and current and speed control loops. In current

^{*} Dr., Space Mechanics and Control Division, INPE - National Institute for Space Research, Av. dos Astronautas, 1758 São José dos Campos, SP, 12227010, Brazil, val@dem.inpe.br

[†] MSc. student, Space Mechanics and Control Division, INPE - National Institute for Space Research, Av. dos Astronautas, 1758 São José dos Campos, SP, 12227010, Brazil, adolfo.graciano@gmail.com.

^{‡‡} Dr., Space Mechanics and Control Division, INPE - National Institute for Space Research, Av. dos Astronautas, 1758 São José dos Campos, SP, 12227010, Brazil, hkk@dem.inpe.br.

control mode the electronics control the mean motor current by means of a feedback error loop in order to follow a commanded reference. A second and external control loop assures speed tracking by giving a reference to the current loop based on the velocity error. Digital filters keep tacho and current noises between acceptable levels. The bearing friction affects current mode, since friction behavior is far from linear, mainly in small, close to zero, angular velocities. Viscous and Coulomb frictions are predominant at high speeds, but a large static friction prevents wheel from starting at low currents. On the other side, in speed mode the current is adjusted by the internal control loop in order to track the commanded velocity, so the friction is compensated by the control. That's the reason why current mode is deprecated in favor of the speed mode. The price to pay is the control's rising time, which is larger in speed mode than in current mode, but still short and acceptable. However, in recent years a dynamic friction model has been proposed, with significant improvements over the preceding models, which suggest that the mechanism behind friction can be mathematically modeled and controlled. The dynamic friction model assumes that there are elastic bristles in the contact surfaces that bends when slipping forces are applied. The bristle behavior mimics the Stribeck effect without the typical discontinuities.

Despite the versatility of this type of control - with only three wheels, aligned with Cartesian axes, one can control and stabilize the satellite attitude - the reaction wheel is itself a complex device. Major problems in RW design are the bearing alignment, motor selection, bearing lubrication, internal degasification, motor control electronics and flywheel balancing¹. RW specification requires deep knowledge of its characteristics and performance. There are few companies that design and deliver RW for space applications, from very small (0.1 Nms) to large ones (20 Nms or higher). Due to its inherent high technology, there are few academic articles that describe RW design and control. Although the wheel output torque is related to the motor current, it is not usual to command a RW by means of only its current (current control mode). In fact they are driven by analog voltage (reference to torque or current) or to serial interface, which exhibit torque, current or speed control. Whatever the RW command be, it requires electronics for closed loop current control. Velocity or speed control uses digital tachometer and a PID control. Torque command is converted to current by means of the flywheel inertia and wheel acceleration. In spite of the control complexity, it is known that these devices present nonlinear behavior, since the output torque is not directly proportional to the current applied to the motor^{1,2}. The non-linearity is caused mainly by the friction torque, which presents spikes in low angular velocity. The friction torque can be modeled by means of a viscous torque proportional to the wheel speed, a constant or Coulomb torque, and a stiction or static friction torque. A continuous Stribeck friction can replace the static friction. The motor current control is affected by those non-linearities and the reaction wheel presents the so-called zero-speed problem, which increases the attitude pointing error. While conventional attitude control techniques can still be employed, the controller performance is affected by the response of the wheel to a greater or lesser degree. Unfortunately the non-linearities present in the wheel derail or at least make it difficult to tune the controller to a particular performance requirement. To overcome this problem, almost all embedded attitude controllers uses the "speed-control mode", rather than the conventional "current control". From the attitude control point of view, the reaction torque is equal to the product of the flywheel's inertia by the angular acceleration, and that means that to control the wheel speed (which is easily done) is equivalent to control the torque (difficult). The price to pay for adopting this strategy is an increase in the operation complexity, a delayed response of the wheel (due to the internal speed controller), and the errors associated from deriving the acceleration of the flywheel from some sort of speed measurement device, like a tachometer, for instance. Even the current control mode may have several adverse effects, also shared by the speed control, such as:

- Communication delay caused by digital processing and serial communication line.

- Noise in the analog control line (typically a reference voltage to current or to speed control).
- Non-linearity, noise and scale factor of some electronic components used in the analog circuits for current control loop, if any.

Because the speed control loop must rely on the current control loop, as shown in the simplified diagram of Fig. 1, a current controlled RW can be preferable under certain circumstances. In this case an accurate mathematical model (if possible) of a current controlled reaction wheel can be a significant step toward having an improvement in the attitude control performance. Thus the objectives of this work are: to establish a mathematical model for the friction in a RW; to evaluate several methods to estimate friction parameters through curve fitting, Kalman and Extended Kalman filtering; to compare those methods; and to check its correctness and convergence. Next sections present the experiments performed with a reaction wheel from SunSpace³ (SSRW), coupled to a single axis air-bearing table at the Simulation Laboratory of INPE (National Institute for Space Research – São José dos Campos, SP, Brazil). The reaction wheel has a maximum capacity of 0.65 Nms, inertia of $1.5 \cdot 10^{-3} \text{ kg m}^2$, maximum angular velocity of 4200 rpm, maximum torque of 0.05 Nm and can be controlled by current or by speed through a serial RS485 interface. The wheel's angular speed is sampled at 10 Hz maximum rate.

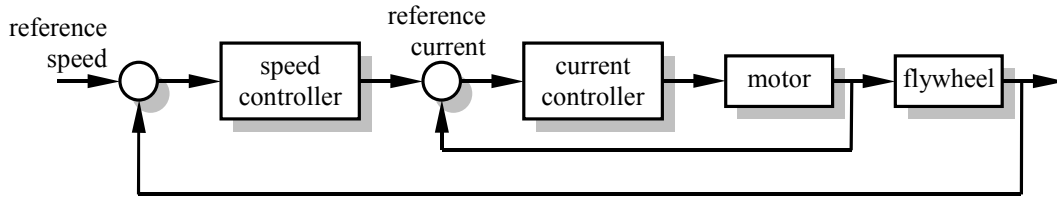


Figure 1. Reaction wheel closed loop controller.

An experiment² with the above mentioned RW was performed using current control mode to stabilize and to point the air-bearing table based on a fiber-optics gyro angular rate measurements. A current control loop with a model compensation controller⁴ was implemented in the control computer which showed small yet significant pointing error during zero-speed crossing.

REACTION WHEEL FRICTION MODEL

A reaction wheel can be modeled by the inertia J_w of the flywheel, a viscous friction b and a Coulomb friction c . The differential equation that describes the motion is²:

$$T_w = J_w \dot{\omega} + b \omega + c \text{sgn}(\omega) \quad (1)$$

where ω is the angular velocity of the wheel and T_w is the motor torque. Neglecting nonlinear effects present in the conversion from current to torque (there is no data concerning these values), one can consider that the torque is linear to the current I :

$$T_w = k_m I \quad (2)$$

where k_m is the torque constant. Some authors consider also a stiction torque that prevents the shaft from departure whenever the motor torque is less than the break-away torque. In order to distinguish stiction from Coulomb, it is accepted that Coulomb is different from zero only during

motion. Stiction exhibit a high variation from still to motion, causing discontinuity in the dynamic equation. This behavior can be avoided by adopting the Stribeck effect that mimics the stiction torque but still keeping the necessary continuity condition. After including the Stribeck torque, the differential equation is changed to⁵:

$$T_w = J_w \dot{\omega} + b \omega + c \operatorname{sgn}(\omega) + (s - c) \exp\left|\omega / \omega_s\right|^\delta \operatorname{sgn}(\omega) \quad (3)$$

in which s is the break-away torque, ω_s is known as the Stribeck velocity, and δ is the Stribeck exponent, usually adopted as unit or 2.

In spite of these already complex models, friction is still loosely understood, since there is experimental evidence that not only the velocity plays an important role, but also the displacement in very small velocities. So as to include this effect it was suggested that a dynamic friction model should be considered as representative of the phenomenon. One of the proposed models⁵ states that friction can be seen as a large number of deflecting bristles interacting with each other in the contact surfaces. In the LuGre model the dynamic friction is given by the differential equation:

$$\dot{z} = \omega - \sigma_0 \frac{|\omega|}{g(\omega)} z \quad (4)$$

where z stands for the mean deflection of the bristles, in a spring-like fashion. Of course z is non-observable, which means that there is no way one can measure this variable, yet it can still be estimated. The friction torque can be modeled by:

$$T_f = \sigma_0 z + \sigma_1 \dot{z} + b \omega \quad (5)$$

where σ_0 is the stiffness and σ_1 is the damping coefficient of the bristles. The $g(\omega)$ function accounts for the Stribeck effect:

$$\sigma_0 g(\omega) = c + (s - c) \exp\left|\omega / \omega_s\right|^\delta \quad (6)$$

It can be shown⁶ that the dynamic friction model is identical to the wheel's equation in Eq. (3), whenever the bristle deflection is constant (i. e. in steady state, with $\dot{z} = 0$). Canudas de Wit and Lischinsky⁷ applied the dynamic friction model to a DC motor attached to a flywheel through a gear train. Shaft position and velocity were measured with a high precision 120,000 optical encoder, sampled at 200 Hz. That is necessary as the bristle dynamics, according to Eq. 4, presents quick variation at very low speed and position, which can only be detected with such high sample rate and angular displacement resolution. In fact, it is possible to state that friction dynamics can be observed only in these conditions of motion: starting or stopping. The obvious conclusion is that the experimental procedures shall take into account the friction parameter to be estimated, in order to put into evidence its change during experiment. To do so, several experiment were carried out with the Sun Space RW in order to highlight one or more parameters simultaneously. These tests are described in next sections.

Viscous and Coulomb Coefficients

To estimate the viscous friction coefficient b , the wheel was accelerated up to a given rate, and then left free till complete stop, as shown in Fig. 2. The solution of differential motion equation (1) in this situation, neglecting the bristle contribution and the Stribeck effect, leads to:

$$\omega = \omega_o \frac{\exp(-\beta t) - \exp(-\beta t_f)}{1 - \exp(-\beta t_f)} \quad (7)$$

where $\beta = b / J_w$, ω_o is the initial decay rate and t_f is the decay time. Through least squares error fitting b results equal to $5.16 \cdot 10^{-6}$ Nms, $c = 0.8795 \cdot 10^{-3}$ Nm, with $\omega_o = 3495$ rpm and $t_f = 333.3$ s, if one considers that $J_w = 1.5 \cdot 10^{-3}$ kg m² according to the manufacturer. The theoretical and measured curves were superimposed in Fig. 3, where no visible differences can be seen. The maximum error after model fitting is 15 rpm, or 0.5%, approximately.

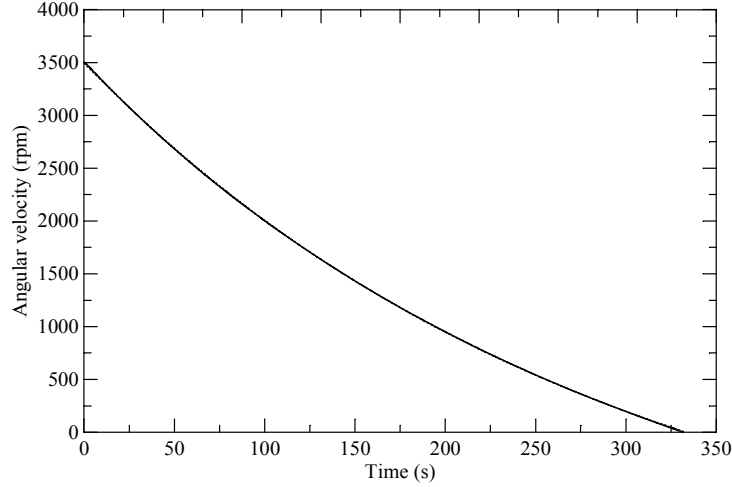


Figure 2. Angular velocity decay due to RW bearing friction.

The motor constant, k_m , can be estimated by measuring the steady state of the angular velocity for a given commanded current. The envisaged experiment to emphasize k_m was to command a given current in the reaction wheel and measure its steady-state velocity. Since the motor torque is counter-balanced by the friction torque in steady state, it is:

$$k_m I = b \omega_w + c \operatorname{sgn}(\omega_w) \quad (8)$$

The result is shown in the solid curve of Fig. 3, while the dashed one shows the model obtained from the steady state solution, adjusted after minimizing the mean square error. Since b and c are known, k_m can be calculated with any of them, which provide, respectively 0.0277 and 0.0251 Nm/A. The difference is probably due to uncertainty in the knowledge of inertia, in addition to measurement errors. The maximum model error occurs when the wheel starts moving from rest. The region around zero-speed where the wheel does not respond to the commanded current (between -38 to 38 mA), is a dead zone caused by the stiction torque. The Stribeck effect can be roughly seen in the figure, at the ending of the dead zone.

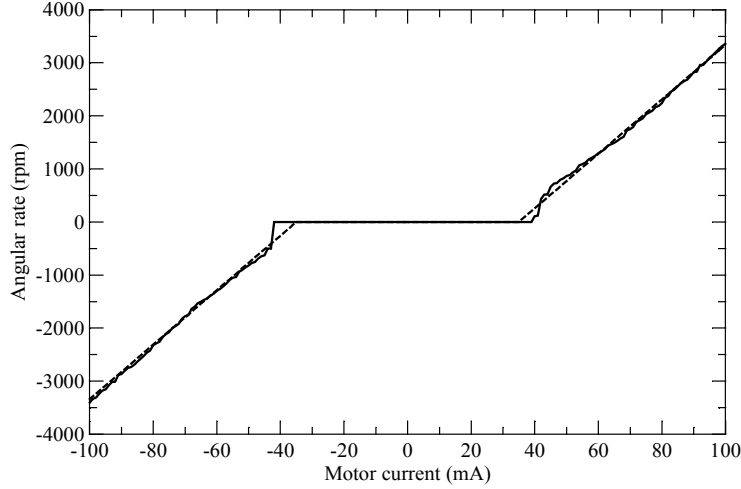


Figure 3. Mathematical model and measured data of RW speed in steady state.

The dead zone can be modeled by a saturation function when the angular velocity is equal to zero, thus resulting for the dynamic equation:

$$\begin{cases} I k_m = J_w \dot{\omega} + b \omega + [c + (s - c) \exp|\omega / \omega_s|^\delta] \text{sgn}(\omega), & \text{if } \omega \neq 0 \\ I k_m - s \text{sat}(I k_m / s) = J_w \dot{\omega}, & \text{if } \omega = 0 \end{cases}, \quad (9)$$

where $\text{sat}(x)$ is the saturation function defined by:

$$\text{sat}(x) = \begin{cases} x, & \text{if } -1 < x < 1 \\ -1, & \text{if } x \leq -1 \\ 1, & \text{if } x \geq 1 \end{cases} \quad (10)$$

Stribeck parameters

Once a good preliminary estimate of the viscous and Coulomb coefficients were obtained, the reaction wheel was submitted to 5 sinusoidal profiles in current mode, with amplitude ranging from 0.1 to 0.2 A and bias of -0.05 A, periods of 30, 120 and 480 s with three cycles. The telemetered speed and current was later processed with a Kalman filter in order to estimate Coulomb, Stribeck, viscous and also the motor torque constant⁸. The previous calculated values of c and b were fed in the Kalman filter as initial guesses to assure convergence. All the current profiles presented similar results. Fig 4 shows the ratio c/J_w and s/J_w of the Coulomb and Stribeck coefficients during one of the tests (0.1 A amplitude and 30 s period). The Stribeck velocity, ω_s , was adopted as 25 rad/sec, based on Fig 3, and with an exponent $\delta = 2$. However, there is some indirect evidence that this Stribeck velocity is over estimated by a factor as large as 5 or even higher. Since the Stribeck effect quickly vanishes at intermediate speeds, it is expected that the difference in ω_s shall not be relevant. However this fact is still to be proven. Considering the wheel inertia of $J_w = 1.5 \cdot 10^{-3} \text{ kgm}^2$ the Coulomb and break torque result respectively $c = 0.848 \pm 0.015 \cdot 10^{-3} \text{ Nm}$ and $s = 0.964 \pm 0.008 \cdot 10^{-3} \text{ Nm}$ after filtering. Fig. 5 presents the filter convergence of the ratio between the torque constant and the wheel inertia, k_m/J_w , which yield $k_m = 24.968 \pm 0.001 \cdot 10^{-3} \text{ Nm/A}$. This parameter presented a tiny variation during filtering, which means that it was well

determined. The viscous coefficient also presented small variations (not shown in figure), but its final value of $b = 1.49 \pm 0.55 \cdot 10^{-6}$ Nms was lower than the preceding one computed by curve fitting.

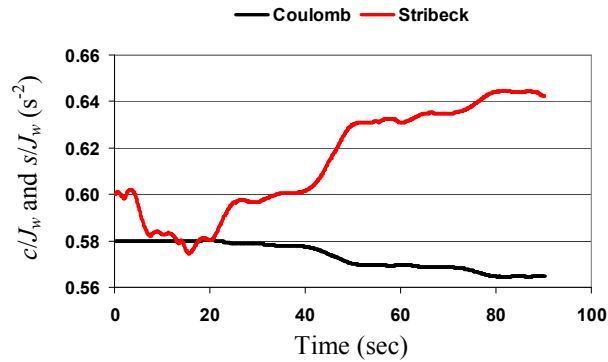


Figure 4. Kalman filtering of the experimental data (Coulomb and Stribeck coefficients)

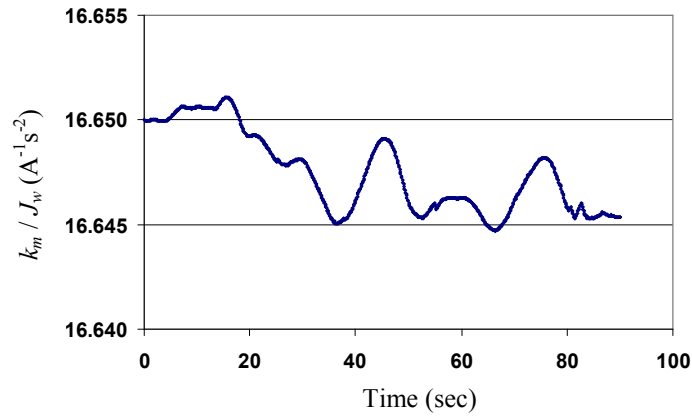


Figure 5. Motor torque constant k_m / J_w .

The measured and estimated values for wheel's angular velocity are shown in Fig. 6. It can be noted that there is an almost perfect match between the model and measured data. Residuals of the estimated angular velocity remain below 5 rpm.

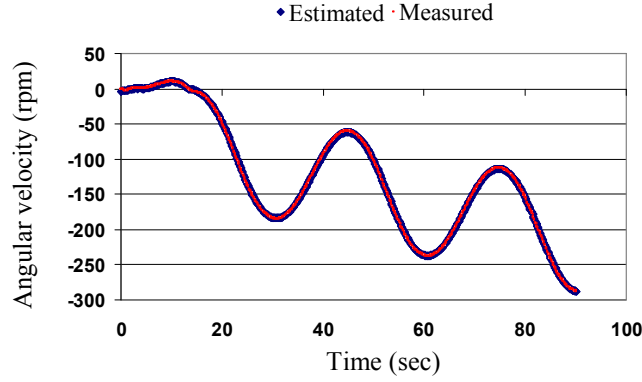


Figure 6. Kalman filtered results from commanded current profile

Extended Kalman filter

The friction model up to this point assures a good phenomenon approximation, enough, for instance, to improve the wheel response with a non-linear control. Carrara⁹ applied a simplified friction model, with Coulomb and viscous friction only, to a Dynamic Model Compensator (DMC) control for the SSRW reaction wheel. This simple model was able to reduce the attitude error of a one-axis bearing table during zero velocity crossing from 2 degrees (without DMC) to 0.2 degrees, although some low velocity effects are not present in this model, like Stribeck or LuGre dynamic friction. So, it appeared to be a good enhancement to make the model still better by adding these effects. Stribeck, as shown in the preceding section, can be easily estimated by batch least squares or Kalman filtering. However due to the high rate of change in the non-observable bristle deflection, the stiffness σ_0 and the damping coefficient σ_1 of the bristles are difficult to estimate, unless the velocity of the wheel could be measured with high precision and high sampling rate, as in the work of Canudas de Wit and Lischinsky⁷. Prior trials to estimate σ_0 and σ_1 by Kalman filtering for the SSRW failed due to the low resolution of the wheel's angular velocity and low sampling rate. So a simulation case was performed in order to check if the Kalman filter solution converges to the true values when better still realistic conditions were met in a reaction wheel.

It is worth to say that the excitation signal should be carefully selected in order to stimulate the desired parameter of the model, otherwise filter divergence may occur. To show the parameter σ_0 , for example, it is suggested⁶ that the control signal must be a ramp in the form $I = \varepsilon t$, where $\varepsilon > 0$ is very small. σ_1 has proven yet more difficult to estimate, although a sensitivity analysis could be made so as to find out the input signal that intensifies the observation of this parameter. A possible method is described in Frank¹⁰. So it is assumed that σ_1 is known, and the filtering process can proceed.

The following values were adopted in the simulation: $c = 0.5 \cdot 10^{-3}$ Nm, $s = 0.66 \cdot 10^{-3}$ Nm, $b = 6.4 \cdot 10^{-6}$ Nms, $\sigma_0 = 2.0$ Nm/rd, $\sigma_1 = 3.0 \cdot 10^{-3}$ Nms/rd, $\omega_s = 0.4$ rd/s, $\delta = 2$, $k_m = 5.0 \cdot 10^{-3}$ Nm/A and $J_w = 2.3 \cdot 10^{-3}$ kgm², based in a similar work of a reaction wheel control¹¹.

An Extended Kalman Filter (EKF) was used to estimate the wheel angular velocity ω and the stiffness of the bristles σ_0 , with initial condition $\omega = 0$ and $\sigma_0 = 0.5$ Nm/rd. The initial covariance matrix, dynamic noise and measurement noise were taken respectively as $P = \text{diag}[1, 16]$, $Q =$

$\text{diag}[10^{-4}, 10^{-2}]$ and $R = 5.2 \cdot 10^{-5}$, which represents high accuracy speed sensor, perhaps not found in a true reaction wheel, but this amount was needed for tuning and to assure the filter convergence. Gaussian noise was added to the angular rate so as to simulate sensor measurements.

The final value of σ_0 after the filtering process was 1.94 ± 0.2 Nm/rd, as shown in Fig. 7. The standard deviation of the measuring residuals is close to the standard deviation of the sensor measurement, as expected due to the fact that the measure noise is far smaller than model noise. Fig. 7 also shows the curves of σ_0 plus and minus the estimated standard deviation.

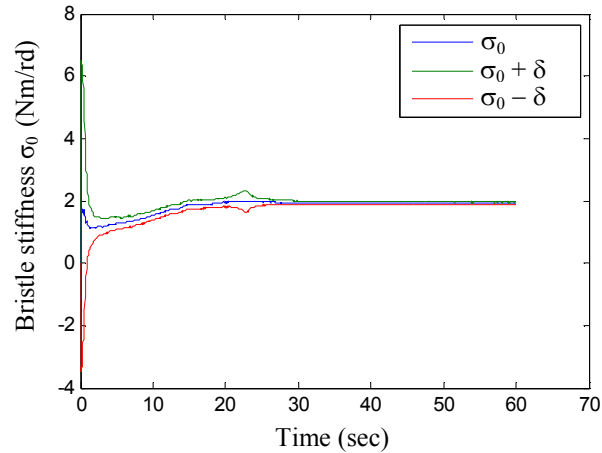


Figure 7. σ_0 estimate by the EKF (δ is the standard deviation)

An increase in standard deviation of the estimated state σ_0 was observed around 20 s of simulation. One possible reason for this trend reversal may be explained at the beginning of the acceleration when the supplied torque becomes greater than stiction torque and the Stribeck effect becomes dominant, as seen in Fig. 8, that shows the wheel's velocity profile.

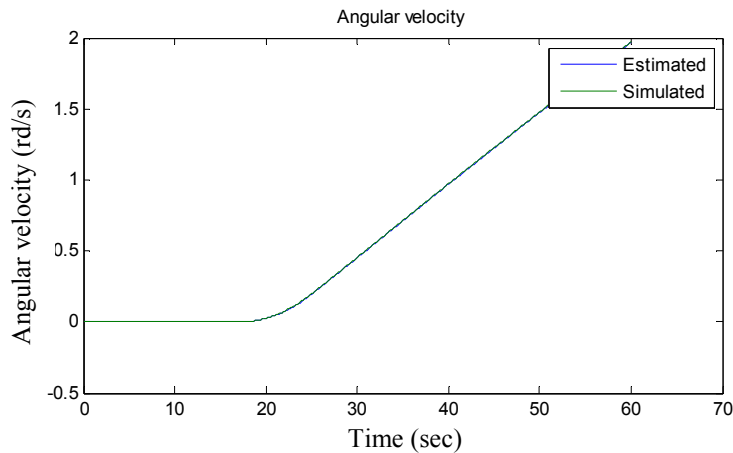


Figure 8. Wheel angular velocity estimative and simulated values.

The non-observable state z estimative is depicted in Fig. 9, as well as its true simulated value. This is, at least, strong evidence that a Kalman filter can estimate the non-observable bristle deflection, provided the necessary conditions are met.

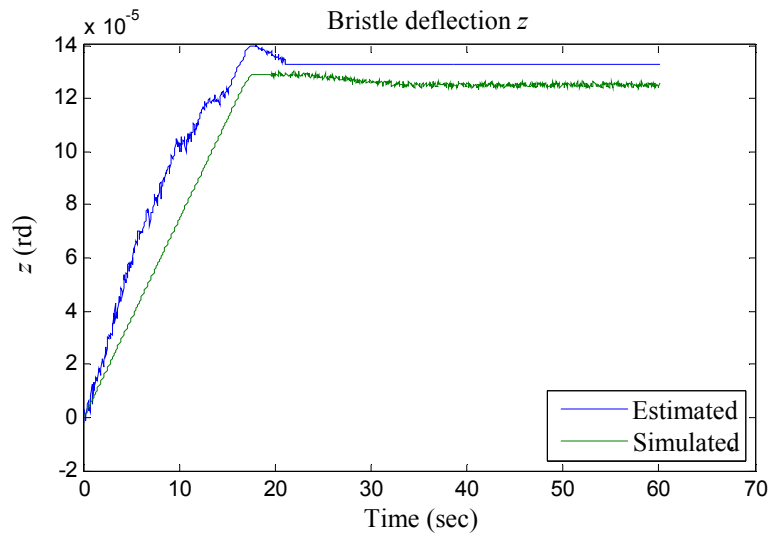


Figure 9. Non-observable bristle displacement z estimated and simulated results.

CONCLUSION

This paper presented a mathematical and computational model for a reaction wheel (RW) manufactured by SunSpace³. Initially the nonlinear model and the viscous and Coulomb friction parameters were obtained with curve fitting of experimental data. Then the model was extended in order to include the break-away force, by using the Stribeck friction model. The break-away torque was estimated by a Kalman filter, with both the Stribeck exponent and velocity previously adopted. The filter also estimated the viscous and Coulomb friction coefficients, which resulted very close to the ones calculated by curve fitting. A LuGre dynamic friction model was then simulated and a EKF was employed in order to estimate the dynamic friction parameters, as well as the non-observable bristle deflection z . The EKF produced good estimates of the wheel speed, bristle stiffness and total friction torque. The residuals from friction torque estimation remained below the minimum necessary to guarantee the accuracy of a non-linear reaction wheel current control. This study shows that an EKF filter can estimate the dynamic LuGre friction model, provided the sensors of angular velocity and current have the high necessary precision.

ACKNOWLEDGMENTS

The authors are grateful to FINEP (Brazilian Foundation for Studies and Projects) through Project SIA-Fundep 11382*3.

REFERENCES

¹ Wertz, J.R., "Spacecraft attitude determination and control". London, D. Reidel, 1978. (Astrophysics and Space Science Library).

- ² Carrara, V., Milani, P.G., “One-axis gas bearing table control with gyro and reaction wheel (in Portuguese)”. V *SBEIN - Brazilian Symposium on Inertial Engineering*. Rio de Janeiro, Nov. 2007. <http://www2.dem.inpe.br/val/publicacoes/vsbein031.pdf>.
- ³ Engelbrecht, J.A.A., “User's Manual for the reaction wheel and gyroscope SunSpace subsystem”. *SunSpace*, Matieland, South Africa, 2005. (SS01-106 000).
- ⁴ Carrara, V., “Experimental comparison between reaction wheel attitude controller strategies”. *Journal of Aerospace engineering, Sciences and Applications*, Vol 2, n. 2, 2010. p. 1-9. ISSN 2236-577X.
- ⁵ Olsson, H.; Olsson, H.; Åström, K. J.; Canudas de Wit, C.; Gafvert, M.; Lischinsky, P., “Friction models and friction compensation.” *European Journal of Control*, Vol. 4, No. 3, pp. 176-195, 1998.
- ⁶ Canudas de Wit, C.; Olsson, H.; Åström, K.J.; Lischinsky, P., “A New Model for Control of Systems with Friction”. *IEEE Transactions on Automatic Control*, Vol 40. No. 3, March 1995.
- ⁷ Canudas De Wit, C.; Lischinsky, P., “Adaptive Friction Compensation with Partially Known Dynamic Friction Model”. *International Journal of Adaptive Control and Signal Processing*, Vol 11, p. 65-80, 1997.
- ⁸ Fernandes, D. C.; Kuga, H. K.; Carrara, V; Romano, R. A., “A model for a reaction wheel with estimation of friction parameters by Kalman filtering (in Portuguese)”. Submitted to *VII Congresso Nacional de Engenharia Mecânica – CONEM 2012*. São Luis, MA, Brazil, Aug. 2012.
- ⁹ Carrara, V.; Siqueira, R.H.; Oliveira, D.A., “Speed and current mode strategy comparison in satellite attitude control with reaction wheels”. *Proceedings of COBEM 2011 – 21st Brazilian Congress of Mechanical Engineering*. Natal, RN, Brazil, Oct. 2011.
- ¹⁰ Frank, P. M., “Introduction to System Sensitivity Theory”. *Academic Press*, London, England, 315p., 1978.
- ¹¹ Shenming, G.; Cheng, H., “A Comparative Design of Satellite Attitude Control System with Reaction Wheel”. *Proceedings of the First NASA/ESA Conference on Adaptive Hardware and Systems*. 2006. (AHS'06).